JOURNAL OF Materials CHEMISTRY

Chain folding in poly(ε-caprolactone) studied by small-angle X-ray scattering and Raman spectroscopy. A strategy for blending in the crystalline state

Susan A. Berrill,[a] Frank Heatley,[a] John H. Collett,[a] David Attwood,[a] Colin Booth,*[a] J. Patrick A. Fairclough,[b] Anthony J. Ryan,[b]† Kyriakos Viras,[c] Amanda J. Dutton[d] and Ross S. Blundell[e]

[a]*Department of Chemistry and School of Pharmacy, University of Manchester, Manchester, UK M13 9PL*
[b]*Department of Chemistry, University of Sheffield, Sheffield, UK S3 7UF*
[c]*National and Kapodistrian University of Athens, Chemistry Department, Physical Chemistry Laboratory, Panepistimiopolis, Athens 157 71, Greece*
[d]*Solvay-Interox Ltd, PO Box 7, Baronet Road, Warrington, UK WA4 6HB*
[e]*Sanofi-Winthrop Research, Alnwick, Northumberland, UK NE66 2JH*

Received 9th November 1998, Accepted 18th February 1999

Samples of poly(ε-caprolactone), including narrow fractions obtained by preparative gel permeation chromatography (GPC), were characterised by analytical GPC and ^{13}C NMR spectroscopy. The crystallised samples were investigated by small-angle X-ray scattering to obtain lamellar spacings and by low-frequency Raman spectroscopy to obtain LAM-1 frequencies. Together the two methods gave a reliable estimate of the critical stem length for chain folding in poly(ε-caprolactone) crystallised at room temperature or below, *i.e.* 15 chain units [CL, $OCO(CH_2)_5$] equivalent to 105 chain atoms. A necessary requirement for molecular blending of block copolymers of ε-caprolactone and ethylene oxide with crystalline high molar mass poly(ε-caprolactone) is cocrystallisation. Hence it was concluded that a safe lower limit for successful blending is a poly(ε-caprolactone) block of 20 CL units.

Introduction

Poly(ε-caprolactone) [poly(CL), $CL=OCO(CH_2)_5$] has potential as a biodegradable polyester for use in solubilisation and/or encapsulation of drugs.[1] Its biodegradation is based on hydrolysis of the ester linkages, which in turn requires permeation of water into the polymer. Since the polymer is highly hydrophobic, a number of strategies have been reported for enhancing water permeation. These include statistical copolymerisation with less hydrophobic comonomers (*e.g.* DL- or L-lactide),[2] block copolymerisation with a hydrophilic comonomer (*e.g.* ethylene oxide),[3] and blending with a hydrophilic polymer or copolymer (*e.g.* with Synperonic-PE 61, an oxyethylene/oxypropylene block copolymer).[4]

Our immediate interest is in using poly(CL) for encapsulation, for which purpose blending high molar mass poly(CL) with a second polymer or copolymer is attractive. However, blending is complicated by two factors. One is the well-known thermodynamic immiscibility of polymers in the absence of specific attractive interactions, which means that most blends are at best mechanically mixed, and so are heterogeneous on a local scale.[5] The second is the crystallinity of poly(CL),[6–8] with the consequent exclusion of other polymers from the crystalline regions. Of course crystallinity in a polymer can be an advantage, since it is a source of mechanical strength in a material.

Recently we have sought to define the requirements for a stable system based on crystalline high molar mass poly(CL) blended with diblock poly[ε-caprolactone-*block*-poly(ethylene oxide)]. Compatibility with the crystalline poly(CL) was to be ensured through cocrystallisation of the poly(CL) block of the copolymer. Given cocrystallisation, the poly(oxyethylene) [poly(E), $E=OCH_2CH_2$] block must be sited in the interlamellar region of the stacked crystal lamellae, thus providing pathways for permeation of water into the bulk of the material. The rate of permeation could then be controlled by varying the proportion of poly(E) in the copolymer.

In considering such a strategy, it was apparent that best results would be expected if the copolymers to be blended were small. This in itself, by promoting the entropy of mixing, would enhance miscibility. Random incorporation of many short poly(CL) blocks into a lamellar crystal would also mean an even distribution of short poly(E) blocks at the lamellar surfaces. Equally importantly, the preparation of block copolymers by sequential anionic polymerisation is relatively straightforward for short blocks. This being so, it was desirable to define the minimum length of a poly(CL) block that would ensure cocrystallisation, since very short poly(CL) blocks would be rejected from the crystal.

Lamellar spacings in poly(CL) were measured many years ago by Perret and Skoulios using small-angle X-ray scattering (SAXS).[9] The lamellar spacing for a crystallised sample of a high molar mass poly(CL) was found to be 165 Å, this being the stem length between chain folds. Their investigation of the spacings for short chains showed that this value was closely approached when the poly(CL) chain length reached 30 CL units (here denoted CL_{30}). However, in their experiments the approach to the limiting value was gradual, probably as a consequence of the chain length distribution in the fractions. It seemed possible that the limit might be reached at a shorter poly(CL) chain length. As described in this report, related experiments using fractions with very narrow chain length distributions showed this to be so. Investigation of the longitudinal acoustic mode (LAM) vibration by low-frequency Raman spectroscopy provided useful confirmatory evidence for this conclusion, since the single-node longitudinal vibration

†Also CCLRC Daresbury Laboratory, Warrington, UK WA4 4AD.

(LAM-1) is directly related to the crystal-stem length, and so guards against a false conclusion from SAXS data caused by crystal-stem tilting in the lamella.[10]

Experimental

Polymers: preparation and characterisation

Three poly(CL) samples with number-average molar mass in the range $M_n = 2000$–4000 g mol^{-1} (chain length $n = 17$–35 CL units) were selected from the range produced by Solvay Interox, Widnes, UK. These samples had fairly narrow chain length distributions ($M_w/M_n = 1.2$–1.4). A fourth high molar mass polymer ($M_n \approx 80000$ g mol^{-1}, $M_w/M_n = 1.5$) was also examined in order to fix an upper limit to the lamellar spacing. The anionic polymerisation of these samples was initiated by butanediol. In what follows we denote polymers as P-CL_n, where n is the number-average chain length in CL units. Polymer fractions (see below) are denoted F-CL_n.

A polymer of low molar mass ($M_n \approx 450$ g mol^{-1}, P-CL_4) was prepared in our laboratory, starting from pentanediol. ε-Caprolactone (Solvay Interox) was stirred overnight with 2,4-diisocyanato-1-methylbenzene (2 wt%, Fluka AG), distilled under reduced pressure (140 °C, 15 mm Hg) directly onto calcium hydride (Fischer Scientific), and then redistilled onto activated type 4 Å molecular sieves for storage. Immediately before use, pentane-1,5-diol (Lancaster Chemicals) was dried by warming *in vacuo* for 24 h before being distilled at reduced pressure. The catalyst, stannous 2-ethylhexanoate (Sigma), was used as provided. For polymerisation, pentanediol (3.5 g, 0.03 mol) and ε-caprolactone (11.6 g, 0.1 mol) were syringed into a dry ampoule containing a magnetic stirrer. After addition of a drop of the catalyst, the contents of the ampoule were degassed, and the reaction mixture then stirred in a sand bath at 160 ± 5 °C for 7 h. Characterisation by ^{13}C NMR spectroscopy and analytical GPC gave $M_n = 450$ g mol^{-1} and $M_w/M_n = 1.26$.

Polymer P-CL_4 was separated by preparative gel permeation chromatography (preparative GPC) into fractions with very narrow chain length distributions. A single 500 Å Styragel column (120 cm × 57 mm, Waters Assoc.) was used. Polymer (0.5 g) in 20 cm^3 toluene was injected into the solvent stream (flow rate 10 cm^3 min^{-1}) at room temperature. Emergence of sample was detected by differential refractometry, upon which 20×50 cm^3 volumes were collected. The fractions of polymer were isolated by evacuation of solvent (24 h, 10^{-3} mm Hg, room temperature). In all, twenty fractions were collected, many very small, and just five were used in further work.

The polymers and fractions were analysed by GPC (for distribution width) and ^{13}C NMR spectroscopy (for number-average chain length). Two GPC systems were used. System A comprised three PLgel columns (Polymer Laboratories, 1 × 500 Å and 2 × mixed B) used with tetrahydrofuran (THF) eluent (room temperature, 1 cm^3 min^{-1}, dodecane flow marker). Samples were injected as 2 g dm^{-3} solutions *via* a 100 mm^3 loop, and detected by differential refractometry. Universal calibration[11] was with polystyrene standards and the Mark–Houwink constants for poly(styrene) ($K = 0.932 \times 10^{-4}$, $a = 0.740$) and poly(ε-caprolactone) ($K = 1.395 \times 10^{-4}$, $a = 0.786$) in THF at room temperature advocated by Schindler *et al.*[12] System B comprised four PLgel columns (all mixed E) used with chloroform eluent (room temperature, 0.3 cm^3 min^{-1}), other features being similar to those of System A. System B provided excellent resolution in the low-molar-mass range. As examples, GPC curves obtained using systems A and B for analysis of fraction F-CL_{14} are shown in Fig. 1. The curve from System A indicates a narrow chain length distribution (polydispersity index $M_w/M_n \approx 1.02$) while that from System B shows the sample to consist predominantly of three oligomers. Values of M_w/M_n are listed in Table 1.

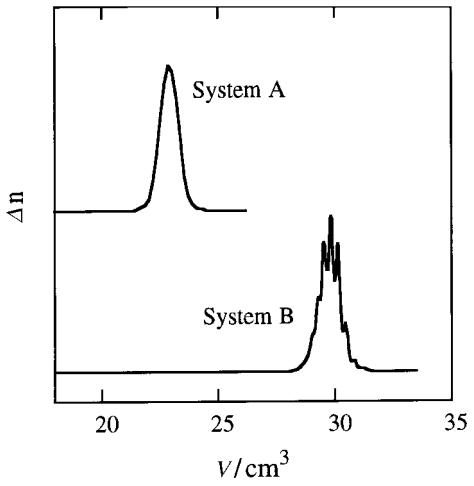

Fig. 1 GPC curves obtained for poly(ε-caprolactone) fraction F-CL_{14} using GPC systems A and B, as indicated.

Table 1 Molecular characteristics of the poly(CL) samples

Sample	M_w/M_n[a] (GPC)	M_n/g mol^{-1} (NMR/GPC)
Polymers		
P-CL_{19}	1.26	2200
P-CL_{25}	1.41	2900
P-CL_{38}	1.41	4300
P-CL_{700}	1.46	80000[b]
Fractions		
F-CL_5	1.02	590
F-CL_9	1.02	1060
F-CL_{11}	1.02	1300
F-CL_{14}	1.02	1630
F-CL_{16}	1.02	1800

[a] M_w/M_n to ±0.01, M_n to ±2%. [b] Value supplied by Solvay Interox.

^{13}C NMR spectra were obtained using a Varian Associates Unity 500 spectrometer operated at 125.8 MHz. Samples were dissolved in deuterochloroform, concentration 0.1 g cm^{-3}. Analysis of the NMR spectra varied slightly depending on the initiator used in preparation of the sample. Both commercial polymers and fractions conformed to the general formula CL*CL_xICL_xCL*, where

$$\underset{\text{a b c d e f}}{\text{CL} = \text{CO}\cdot\text{CH}_2\text{CH}_2\text{CH}_2\text{CH}_2\text{CH}_2\text{O}}$$

$$\underset{\text{a b c d g h}}{\text{CL}^* = \text{CO}\cdot\text{CH}_2\text{CH}_2\text{CH}_2\text{CH}_2\text{CH}_2\text{OH}}$$

$$\underset{\text{i j j i}}{\text{I} = \text{OCH}_2\text{CH}_2\text{CH}_2\text{CH}_2\text{O}} \text{ or } \underset{\text{f e k e f}}{\text{OCH}_2\text{CH}_2\text{CH}_2\text{CH}_2\text{CH}_2\text{O}}$$

The chemical shifts (δ) for the carbons as labelled are listed in Table 2: as indicated, those in the spectra of the low molar mass samples varied somewhat because of end effects. With the exception of the resonance of the CO carbon (a), which had a low integral because of its longer relaxation time and lower NOE, the integrals of equivalent carbons were identical within experimental error. The sum of integrals of all resonances (except a), appropriately related to the sum of integrals of resonances from end group and initiator residue carbons, gave the values of M_n listed in Table 1 for the polymers and for fractions F-CL_{14} and F-CL_5. There was no evidence of ring formation.

Because of the small amounts of material available, only two fractions were characterised in this way. Molar masses of other fractions were obtained by use of analytical GPC (System

Table 2 ^{13}C NMR chemical shifts ($CDCl_3$)

Carbon	δ/ppm
a	173.5
b	34.1
c	25.5
d	24.5
e	28.3
f	64.1
g	32.3
h	62.5
i	68.9
j	21.7
k	22.2

Range: ± 0.1 ppm for polymers ($M_n > 1000$ g mol^{-1}); ± 0.5 ppm for fractions ($M_n < 1000$ g mol^{-1}).

A) as follows. (i) Values of molar mass at the peak of the GPC curve (M_{pk}) were calculated as $M_{pk} = M_n(M_w/M_n)^{1/2}$, with M_n from NMR spectroscopy and M_w/M_n from GPC. This provided a common basis for plotting the data for the polymers and fractions. (ii) Note was taken of the effect of hydrogen bonding of THF with the OH end groups of the samples. From comparison of the elution of low molar mass polyethylene glycols and their dimethyl ethers, this effect was found to decrease the elution volume consistent with an approximate correction to M_n of each sample of 140 g mol^{-1}. The resulting calibration curve is shown in Fig. 2. With acceptable scatter, the three commercial samples and the two fractions fit to a common curve. Accordingly values of M_{pk} for the fractions were obtained from their elution volumes in System A and converted to values of M_n by reversing the procedures (i) and (ii). These values, for fractions F-CL_9, F-CL_{11} and F-CL_{16}, are included in the last column of Table 1.

X-Ray scattering

Measurements were made on beamline 8.2 of the SRS at the CCLRC Daresbury Laboratory, Warrington, UK. The camera was equipped with a multiwire quadrant detector (SAXS) located 3.5 m from the sample position and a curved knife-edge detector (WAXS) that covered 70° of arc at a radius of 0.3 m. Samples were sealed into TA Instruments DSC pans containing a 0.75 mm brass spacer ring and fitted with windows made from 25 μm thick mica. The loaded pans were placed in the cell of a Linkam DSC of single-pan design, which could be heated and cooled to allow melting and recrystallisation of the samples. The scattering pattern from an oriented specimen of wet collagen (rat-tail tendon) was used to calibrate the SAXS detector, and high-density polyethylene and an NBS silicon standard were used to calibrate the WAXS detector. The data acquisition system had a time-frame generator which collected the SAXS/WAXS data in 6 s frames separated by a wait-time of 10 μs. Parallel plate ionisation detectors placed before and after the sample cell recorded the incident and transmitted intensity. The experimental data were corrected for background scattering (subtraction of the scattering from the camera, hot stage and an empty cell), sample thickness and transmission, and for any departure from positional linearity of the detectors. Since the samples crystallised with small domains randomly arranged the resulting pattern was analogous to that of a powder, and all orientations were adequately sampled in the one-dimensional experiment. Further details of the equipment and methods can be found elsewhere.[13–16]

Low-frequency Raman spectroscopy

Raman scattering at 90° to the incident beam was recorded by means of a Spex Ramalog spectrometer fitted with a 1403 double monochromator plus a third (1442U) monochromator operated in scanning mode. The light source was a Coherent Innova 90 argon-ion laser operated at 514.5 nm and 300 mW. Typical operating conditions were bandwidth 0.8 cm^{-1}, scanning increment 0.05 cm^{-1}, integration time 6–12 s. The frequency scale was calibrated by reference to the 9.4 and 14.9 cm^{-1} bands in the spectrum of L-cystine. Samples in a thin-wall capillary were melted and recrystallised at room temperature (approximately 20 °C). Spectra were recorded with the samples at various temperatures in the range 22 to −100 °C, controlled to ±1 °C by means of a Harney-Miller cell (Spex Industries).

Results and discussion

The WAXS patterns obtained were as expected for crystalline poly(CL), *e.g.* strong reflections at Bragg angle $\theta = 10.4°$ and 11.6°, and weaker reflections also in keeping with expectation.[6]

Lamellar spacings from SAXS

Representative SAXS patterns are shown in Fig. 3 and 4. Fig. 3 shows a time-resolved relief diagram of SAXS data obtained during a melting–recrystallisation cycle (ramp rate = 10 °C min^{-1}) for sample P-CL_{25}. Intensity is plotted against temperature and scattering vector $q = (4\pi/\lambda)\sin\theta$, where the wavelength $\lambda = 1.54$ Å. In this notation, the lamellar spacing is given by Bragg's Law in the form $d = 2\pi/q^*$, where q^* is the value of q at the first-order peak. Fig. 4 shows the scattering

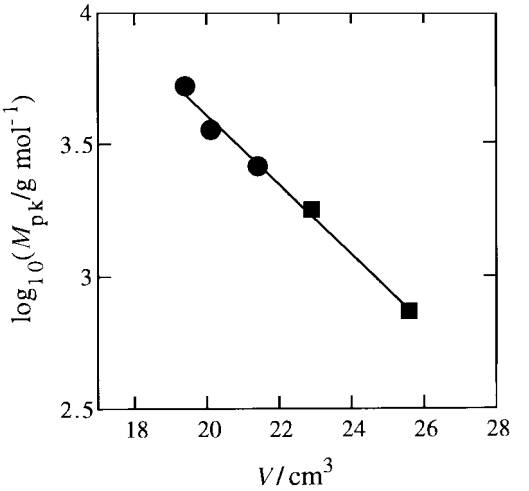

Fig. 2 GPC calibration curve (System A) for poly(ε-caprolactone) (●) polymers and (■) fractions.

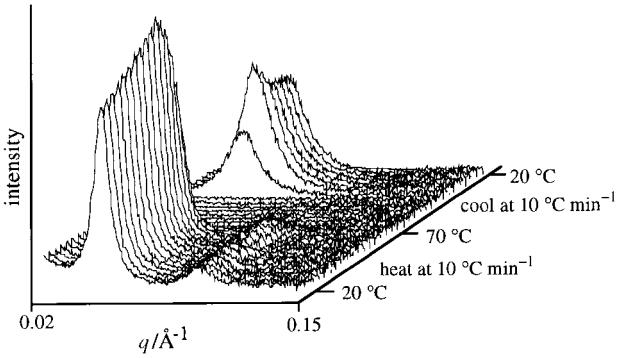

Fig. 3 Time-resolved relief diagram of SAXS data obtained during a melting–recrystallisation cycle (ramp rate = 10 °C min^{-1}) for sample P-CL_{25}. Intensity (arbitrary scale) is plotted against temperature and scattering vector $q = (4\pi/\lambda)\sin\theta$, where $\lambda = 1.54$ Å and θ is the scattering angle.

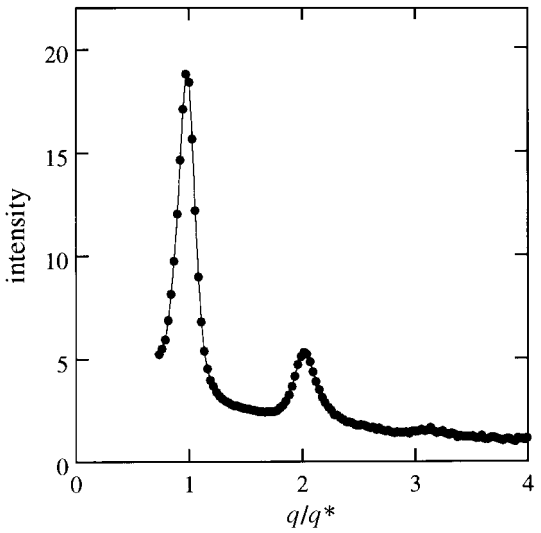

Fig. 4 Scattering intensity (arbitrary scale) plotted against the ratio q/q^* for fraction F-CL_{14} at 10 °C. The parameter q^* is the value of q at the first-order peak: in this case $q^* = 0.055$ Å^{-1}.

intensity plotted against the ratio q/q^* for sample F-CL_{14} at 10 °C, at which temperature $q^* = 0.055$ Å^{-1}.

Values of the lamellar spacing are listed in Table 3 and plotted against chain length (in CL units) in Fig. 5. Also plotted in Fig. 5 are the results of Perret and Skoulios.[9] The two data sets are in substantial agreement. The sharp break in the curve in the present results at chain length 15 CL units and $d = 129$ Å is attributable to the use of very narrow fractions, $M_w/M_n \approx 1.02$, in this work. The d-spacing of 129 Å corresponds to 8.6 Å per CL unit, which is in keeping with the orthorhombic sub-cell dimension $c = 17.05$ Å or $c = 17.26$ Å (for 2 units per repeat) respectively reported by Chatani *et al.*[6] and Hu and Dorset,[7] and so consistent with the crystal stems being normal to the lamellar end planes.

Table 3 Lamellar spacings for crystalline poly(CL) samples at 20 °C

Sample	d/Å[a]
P-CL_{19}	133
P-CL_{25}	128
P-CL_{38}	128
P-CL_{700}	149
F-CL_{9}	82
F-CL_{11}	103
F-CL_{14}	117
F-CL_{16}	128

[a] d to ±3 Å.

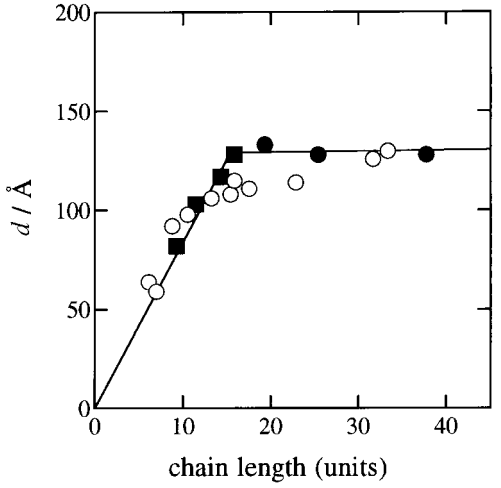

Fig. 5 Lamellar spacing from SAXS (d) *versus* chain length in CL units for poly(ε-caprolactone) (●) polymers and (■) fractions. The open symbols (○) denote the results of Perret and Skoulios.[9] The full lines are drawn through the data points for the present samples.

On the basis of the SAXS data, we conclude that the chain length between folds (crystal stem length) in low molar mass poly(CL) ($M_n < 4500$ g mol^{-1}) crystallised at low temperatures is approximately 15 CL units. Extrapolation of the line established for the lower molar mass fractions to $d = 150$ Å, the value of d measured in this work for the high molar mass sample, would suggest 17 CL units, while extrapolation to $d = 165$ Å (Perret and Skoulios[9]) would take this value to 19 CL units. Values of d reported by Khambatta *et al.*[17] for moderate molar mass poly(CL) ($M_n = 13000$ g mol^{-1}) are near to 150 Å. It seems that a safe lower limit to ensure that a short CL chain will cocrystallise with chain-folded lamellar crystals of high molar mass poly(CL) is 20 CL units, equivalent to 140 chain atoms.

LAM-1 frequency from Raman spectroscopy

The three low molar mass polymers were examined by Raman spectroscopy. Examples of low-frequency (< 100 cm^{-1}) spectra are shown in Fig. 6. There are three prominent bands in each spectrum, the frequencies of which are labelled (i) to (iii) in Table 4. The spectra of the samples P-CL_{25} and P-CL_{38} are essentially identical. The spectrum of P-CL_{19} differs at the lowest frequencies, mainly by the reduced intensity of the lowest frequency band (iii), but with some evidence of splitting. Presumably this is a result of end effects from α,ω-hydroxy-ended chains in predominantly unfolded-chain lamellar crystals.

The LAM-1 band was assigned to band (ii) as follows. Adapting the model of Minoni and Zerbi,[18] the lamellar stack was represented as a one-dimensional crystal, with both chain stems and stem-end groups (chain ends or chain folds)

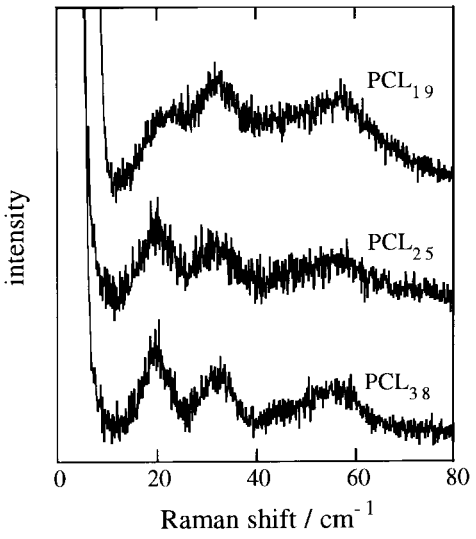

Fig. 6 Low-frequency Raman spectra of poly(ε-caprolactone) samples (as indicated) at 20 °C. The intensity scale and baseline levels are arbitrary.

Table 4 Band frequencies (cm^{-1}) from low-frequency Raman spectra of crystalline poly(CL) samples at 20 °C

Sample	(i)	(ii)	(iii)
P-CL_{19}	58.0	31.8	21.1
P-CL_{25}	57.9	31.6	19.6
P-CL_{38}	57.9	31.8	19.4

Estimated uncertainties: (i) to ±0.2 cm^{-1}, (ii) to ±0.1 cm^{-1}, (iii) to ±0.5 cm^{-1}.

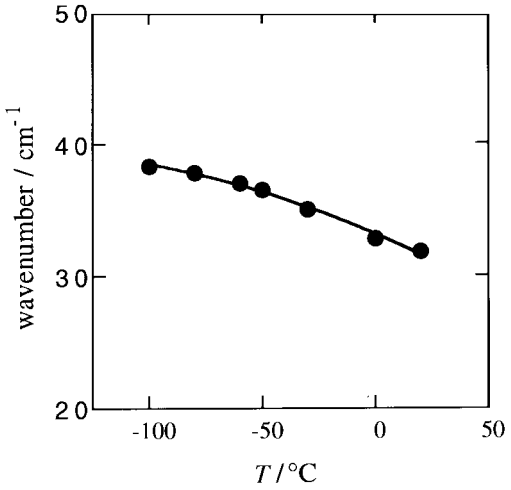

Fig. 7 Temperature dependence of the LAM-1 frequency of poly(ε-caprolactone) P-CL_{19}.

accounted for as point masses with appropriate interactions between them. The SAXS results indicate a spacing equivalent to 15 CL units, equivalent to 105 atoms. In our approximate calculation, the crystal stem was assigned 105 point masses each of 1.895×10^{-25} kg (average value for the CL unit), and the force between chain ends was equated to that typical of a van der Waals interaction ($f_e = 5$ N m^{-1}).[19] Noting the almost *trans*-planar conformation of the poly(CL) chain and the similarity of its packing in the crystal,[6] the force between chain masses was set equal to the value successfully used to model the LAM-1 frequencies of substituted *n*-alkanes ($f_c =$ 420 N m^{-1}). The necessary equations have been given elsewhere.[18,20] The calculated LAM-1 frequency is 29 cm^{-1} compared with 32 cm^{-1} found. Because of hydrogen bonding of hydroxy groups (hydroxy–hydroxy or, more likely, hydroxy–carbonyloxy), it is likely that the chain-end force has a higher value than 5 N m^{-1}, and this would increase the calculated LAM-1 frequency. At the same time, the inertial effect of a chain fold, which is modelled as an end mass, would decrease the LAM-1 frequency. Sensible refinements of the model to account for these effects, using equations already published,[20,21] move the calculated LAM-1 frequency within the range 29–32 cm^{-1} but do not change the assignment.

Further evidence for the assignment of LAM-1 came from the temperature dependence of its frequency. The following results were found for the three bands listed in Table 4:

(i) frequency independent of temperature (within experimental error), allowing it to be assigned to an optical mode;

(ii) frequency dependent on temperature (see Fig. 7), much as expected for LAM-1;[19,22]

(iii) frequency dependent on temperature, allowing it to be tentatively assigned to a bending mode, with the evidence of splitting (see Fig. 6, more obvious at −100 °C) suggesting resolution of orthogonal components.

In that the LAM-1 frequency for a crystalline polymer depends predominantly on crystal stem length, the constant frequency found for the three polymers confirms the conclusion from SAXS that the stem length in those samples is constant. The substantial agreement of the calculated LAM-1 frequency (based on the crystal stem length from SAXS) with the observed frequency is strong confirmatory evidence that the chains in the poly(CL) samples are normal to their lamellar end planes. As noted in the Introduction, this result from Raman spectroscopy guards against the possibility that the lamellar spacing from SAXS is affected by crystal-stem tilting.

Concluding remarks

We are aware that all the samples examined in the present work have an imperfection at the mid-point of the chain. The choice of pentanediol as initiator does not remove this feature, since (on average) the two arms of those chains are symmetrical about the mid-point. While this may affect the crystallinity of the present samples, we find no evidence that it affects the extent of chain folding as quantified by SAXS, nor the LAM-1 frequency from Raman spectroscopy.

We conclude that 20 CL units is a safe lower limit for the CL block length in block copolymers of ε-caprolactone and ethylene oxide if they are to cocrystallise with chain-folded high molar mass poly(ε-caprolactone) and so form blends suitable for encapsulation purposes.

Acknowledgements

We thank Messrs S. K. Nixon and P. Kobryn for help with the experimental work. Sanofi-Winthrop, Alnwick, UK financed a research studentship for SAB. KV had the benefit of a Royal Society of Chemistry Journals Grant for International Authors.

References

1 C. G. Pitt in *Biodegradable Polymers as Drug Delivery Systems*, ed. M. Chasin and R. Langer, Marcel Dekker, London, 1990.
2 E. Piskin, *J. Biomater. Sci., Polym. Ed.*, 1994, **6**, 775.
3 J. Bei, W. Wang, Z. Wang and S. Wang, *Polym. Adv. Technol.*, 1996, **7**, 104.
4 H. Huatan, J. H. Collett, D. Attwood and C. Booth, *Biomaterials*, 1995, **16**, 1297.
5 P. J. Flory, *Principles of Polymer Chemistry*, Cornell U. P., Ithaca, New York, 1953, p. 554.
6 Y. Chatani, Y. Okita, H. Tadokoro and Y. Yamashita, *Polym. J.*, 1970, **1**, 555.
7 H.-L. Hu and D. L. Dorset, *Macromolecules*, 1990, **23**, 4604.
8 V. Crescenzi, G. Manzini, G. Calzolari and C. Borri, *Eur. Polym. J.*, 1972, **8**, 449.
9 R. Perret and A. Skoulios, *Makromol. Chem.*, 1972, **156**, 157.
10 See J. F. Rabolt, *CRC Crit. Rev. Solid State Mater. Sci.*, 1977, **12**, 165.
11 See J. V. Dawkins in *Comprehensive Polymer Science*, *Vol. 1*, *Polymer Characterisation*, ed. C. Booth and C. Price, Pergamon, Oxford, 1989, p. 252.
12 A. Schindler, Y. M. Hibionada and G. C. Pitt, *J. Polym. Sci., Polym. Chem. Ed.*, 1982, **20**, 319.
13 W. Bras, G. E. Derbyshire, A. J. Ryan, G. R. Mant, A. Felton, R. A. Lewis, C. J. Hall and G. N. Greaves, *Nucl. Instrum. Methods Phys. Res., Sect. A*, 1993, **326**, 587.
14 A. J. Ryan, *J. Therm. Anal.*, 1993, **40**, 887.
15 A. J. Ryan, W. Bras, G. R. Mant and G. E. Derbyshire, *Polymer*, 1994, **35**, 4537.
16 W. Bras, G. E. Derbyshire, A. Devine, S. Clarke, J. Cooke, B. U. Komanschek and A. J. Ryan, *J. Appl. Crystallogr.*, 1995, **28**, 26.
17 F. B. Khambatta, F. Warner, T. Russell and R. S. Stein, *J. Polym. Sci., Polym. Phys. Ed.*, 1976, **14**, 1391.
18 G. Minoni and G. Zerbi, *J. Phys. Chem.*, 1982, **86**, 4791.
19 K. Viras, F. Viras, C. Campbell, T. A. King and C. Booth, *J. Phys. Chem.*, 1989, **93**, 3479.
20 C. Campbell, K. Viras and C. Booth, *J. Polym. Sci., Part B, Polym. Phys.*, 1991, **29**, 1613.
21 C. Campbell, K. Viras, A. J. Masters, J. R. Craven, H. Zhang, S. G. Yeates and C. Booth, *J. Phys. Chem.*, 1991, **95**, 4647.
22 K. Viras, T. A. King and C. Booth, *J. Chem. Soc., Faraday Trans. 2*, 1985, **81**, 491.

Paper 8/08718K